JOURNAL OF PROPULSION AND POWER
Vol. 17, No. 4, July–August 2001

Propellant Atomization and Ignition Phenomena in Liquid Oxygen/Gaseous Hydrogen Rocket Combustors

Wolfgang O. H. Mayer,* Blazenko Ivancic,† Axel Schik,† and Ulf Hornung‡
DLR, German Aerospace Center, 74239 Hardthausen a.K., Germany

The mixing and combustion processes in a liquid oxygen/gaseous hydrogen rocket combustor were studied. The research focused on observations of atomization phenomena during steady-state combustion and ignition transients of a rocket engine. Cold-flow atomization as encountered before ignition has been studied using liquid oxygen/gaseous hydrogen and simulation fluids liquid nitrogen/helium. The theoretical assessments show that for binary- and multicomponent systems a transcritical region exists where surface tension is present even at pressures above the critical pressure of one component as long as the critical mixing temperature is not exceeded. Also, hot-fire tests utilizing liquid oxygen/gaseous hydrogen demonstrate the strong influence of the flame on the atomization process. The flame propagation during ignition could be identified by the change of the atomization phenomenology before and during the ignition process.

Nomenclature

d_a	=	outer diameter
d_i	=	inner diameter
P_r	=	reduced pressure
p	=	pressure
T	=	temperature
u, v	=	velocity
μ	=	chemical potential
ρ	=	density
σ	=	surface tension

Subscripts

c	=	chamber
crit	=	critical
gas	=	gas
i	=	specie
liq	=	liquid
s	=	saturation

Introduction

CRYOGENIC rocket engines are used in a number of operational launch vehicles worldwide. The thrust chamber is the core of any liquid rocket engine and consists of injector, combustion chamber, and nozzle. High performance and reusability are the most challenging requirements for future developments requiring large technical advancements for most of the engine components (see Refs. 1 and 2).

The research during the last few years on liquid oxygen/gaseous hydrogen (LOX/GH2) injection has provided an improved understanding of the processes in cryogenic rocket engine combustion chambers (e.g., see Refs. 3–7), although many basic phenomena such as turbulent mixing of propellants cannot be predicted quantitatively. The injection process in cryogenic rocket engines takes place at pressure conditions above the critical pressures of the propellants. During injection the temperatures, however, are under the critical mixing temperature. Therefore, one has to expect a transcritical mixing behavior of the propellants, which this paper discusses. Other important aspects of injection and atomization such as injector design, operating conditions, turbulence, and aerodynamic forces have been treated previously, (see Refs. 4–6 and others).

The principal aim of this paper is to describe and discuss the atomization process of coaxially injected cryogenic propellants (LOX/GH2) under combusting conditions. The different processes are identified by different experimental approaches. After a discussion of the thermodynamic properties of the propellants at high pressure, the results of cold-flow studies and steady-state hot-fire tests are used to explain the main mixing mechanisms. Furthermore, transient mixing phenomena during ignition are described. The study begins with the description of phase equilibrium of pure and multicomponent systems. Cold-flow studies of liquid nitrogen jets are presented where high-pressure subcritical and transcritical phenomena can be observed without the complications of chemical reactions. This is followed by reports on results of steady-state hot-fire test utilizing LOX/GH2. Finally, results of ignition tests in a LOX/GH2 combustor are discussed in detail. The remarkable change in atomization phenomenology is used to identify the flame propagation during ignition.

Before Ignition: Cold Flow

The mixing process of the propellants before ignition takes place is discussed. For this discussion, experimental data from injection tests using the simulation fluids liquid nitrogen (LN2) and He are used.

The possibility of phase equilibrium is a precondition for surface tension between the propellant components. As shown previously (e.g., see Ref. 8), the role of surface tension on atomization predominates. A remarkable change of the atomization mechanisms from wind-induced capillary instability under subcritical conditions to turbulent mixing with expansion under supercritical conditions has been observed and is dependant on local conditions at the jet surface.[6]

In an H2/O2 rocket chamber, the phenomena are very difficult to assess because there are at least three relevant species present (H2, O2, and H2O) as well as high gradients in temperature and mixture ratio. Assuming thermodynamic equilibrium, which may only be valid locally, a phase equilibrium, that is, surface tension, can exist depending on pressure, temperature, and the mixture ratio of the fluids. For a pure component system, a phase equilibrium between liquid and vapor phase exists when the system pressure equals the component vapor pressure and the system temperature equals the respective component boiling temperature.

At the critical point, which is characterized by the critical temperature and pressure, the density of the gas and liquid phase become

Presented as Paper 98-3685 at the AIAA/ASME/SAE/ASEE 34th Joint Propulsion Conference and Exhibit, Cleveland, OH, 13–15 July 1998; received 23 October 1999; revision received 12 February 2001; accepted for publication 12 February 2001.

*Head Propellant Injection Research, Space Propulsion, Lampoldshausen. Senior Member AIAA.
†Aerospace Engineer, Space Propulsion, Lampoldshausen.
‡Student Aerospace Engineering, Space Propulsion, Lampoldshausen.

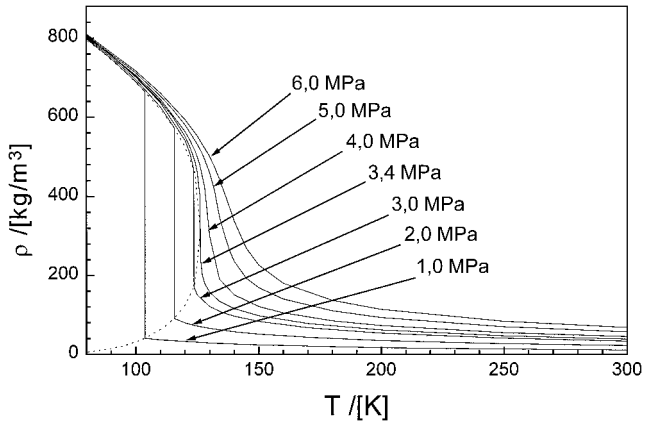

Fig. 1 Phase diagram of nitrogen.

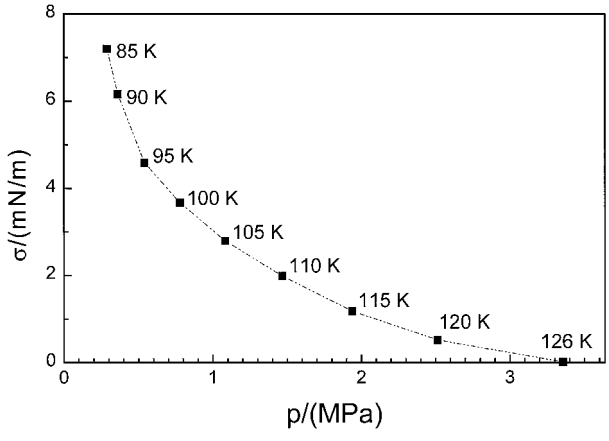

Fig. 2 Surface tension of nitrogen.

the same. The critical pressure of nitrogen is 3.4 MPa. A phase diagram of nitrogen is shown in Fig. 1. One characteristic of exceeding the critical point is that a phase equilibrium no longer exists and that the surface tension goes down to zero (see Fig. 2). Also it can be seen from Fig. 1 that small increases in temperature near the critical point cause large expansions of the fluid. Both exceeding the critical point and small increases in temperature near the critical point strongly influence the mixing mechanics.

Capillary, aerodynamic, and shear forces control atomization. For this study, the surface of a LN2 jet injected into gaseous nitrogen has been visualized. Shadowgraphy has been used as a diagnostic method. For more details of the experimental setup, see Ref. 6. During injection, the system is not in thermodynamic equilibrium. The photographs in Fig. 3 show the observed atomization phenomena. At subcritical conditions (1.0 and 2.0 MPa) the flow is controlled by aerodynamic and capillary forces showing a wavy surface and droplet detachment. In this regime, higher pressure, higher relative velocities, and lower surface tension cause smaller jet surface structures and droplets. At near critical conditions (3.0 MPa) the capillary forces are reduced considerably, but at low injection velocity ($v = 5$ m/s) droplet detachment still occurs. At the higher injection velocity ($v = 10$ m/s), shear forces exceed the capillary forces and the atomization phenomenology appears to be a fluid/fluid mixing process. This is also the case at supercrtical conditions (4.0 MPa), where shear forces and expansion of the jet dominate. An increase of the observed jet contour length scales results from the change of the atomization mechanism.

For a multicomponent system a phase equilibrium can exist between a liquid and a gaseous phase (e.g., see Refs. 9 and 10) if there is a mechanical

$$p_{\text{gas}} = p_{\text{liq}}$$

a thermal,

$$T_{\text{gas}} = T_{\text{liq}}$$

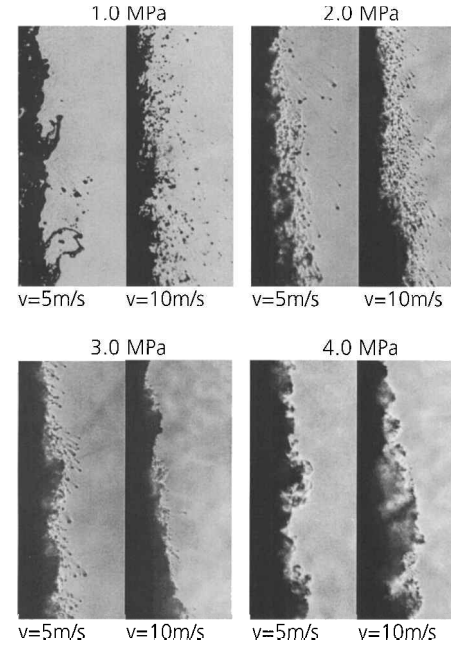

Fig. 3 Shadowgraphs of LN2 jet segments ($T = 105$ K) in gaseous nitrogen environment ($T = 300$ K): $d_{\text{jet}} = 1.9$ mm; image size 3.1 × 7.7 mm; position 8 mm downstream injector; $p_{\text{ambient}} = 1.0, 2.0, 3.0,$ and 4.0 MPa (from left to right and top to bottom), $v_{\text{jet}} = 5$ m/s and 10 m/s (left and right, respectively).

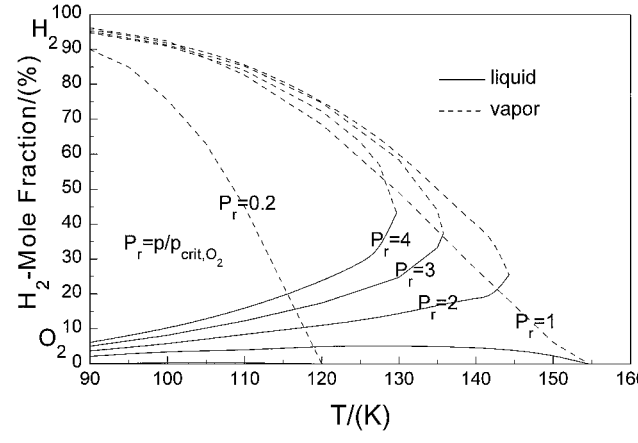

Fig. 4 Phase equilibrium of the O2/H2 system.

and a chemical equilibrium of specie i,

$$\mu_{i,\text{gas}} = \mu_{i,\text{liq}}$$

The phase equilibrium diagram for the two-component system H2/O2 is shown in Fig. 4. For the reduced pressures $P_r = p/p_{\text{crit,O2}}$ ($p_{\text{crit,O2}}$ is 5.04 MPa), the boundaries of the two-phase region are marked. For a given pressure, the solubility of hydrogen in the LOX increases with increasing temperature, and the amount of hydrogen in the gaseous phase decreases. This is the transcritical region. The behavior of the N2/He system shows the same tendencies as the H2/O2 system but has differences in the absolute property values, for example, critical pressures and mixing temperatures. Figure 5 shows a binary mixture (here N2–He) at a given system pressure has a maximum boundary temperature for the existence of a phase equilibrium. This temperature is called the critical mixing temperature.

Above the critical mixing temperature, the species fractions in the gas and liquid phase are identical: The phase boundary disappears and supercritical conditions exist.

Figure 6 shows the critical mixing temperatures as a function of the system pressure for different binary systems. Below the

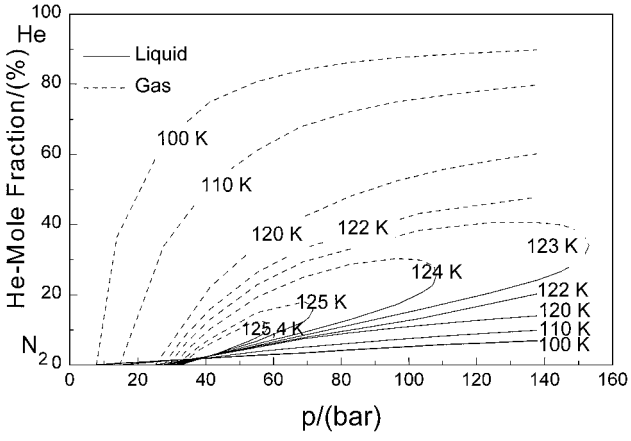

Fig. 5 Phase equilibrium of the N2/He system.

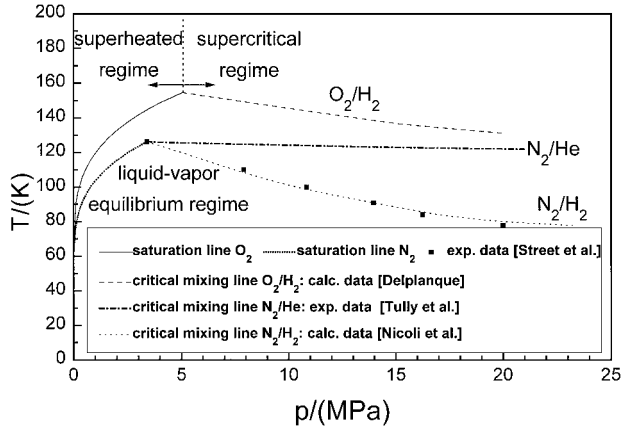

Fig. 6 Critical mixing lines of different binary systems.

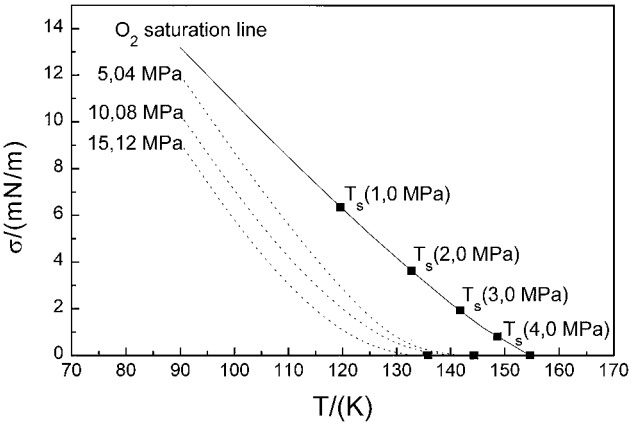

Fig. 7 Surface tension of the binary system H2/O2.

critical mixing temperature, a phase equilibrium with a liquid and a gaseous phase exists. Above this line, supercritical conditions prevail. The general trend is the critical mixing temperatures decrease with increasing pressure. When the Macleod–Sugden correlation (see Refs. 11–13) is used, the surface tension of the binary system H2/O2 is computed, as shown in Fig. 7. The thick line is the saturation line for O2. The dashed lines are constant pressures of the H2/O2 system. Note that even above the critical pressure surface tension is present as long as the critical mixing temperature (145 K) is not exceeded. In typical applications (rocket engine) this temperature margin is very small.

Results of hot-fire tests[5] and cold-flow simulations using LN2 and gaseous He confirm this, (see Fig. 8). The cold-flow simulation tests used a coaxial injector. The baseline injector dimensions are an inner

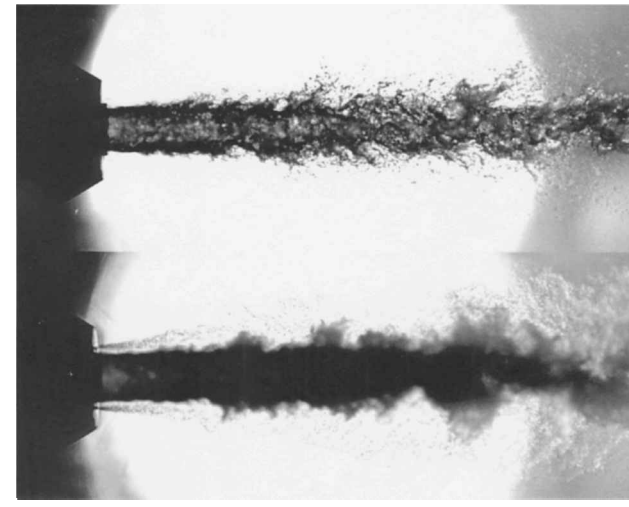

Fig. 8 Shadowgraphs of a coaxial LN2/He jet, T_{LN2} = 97 K, T_{He} = 280 K, v_{LN2} = 5 m/s, v_{He} = 100 m/s, d_{LN2} = 1.9 mm; top picture $p_{ambient}$ = 1.0 MPa, bottom picture $p_{ambient}$ = 6.0 MPa (Ref. 6).

Fig. 9 Coaxial injector.

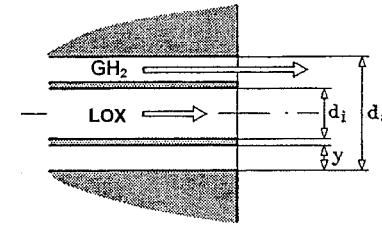

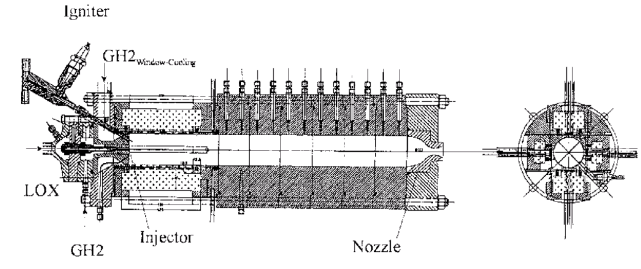

Fig. 10 Windowed single injector model combustor, inner chamber diameter is 50 mm.

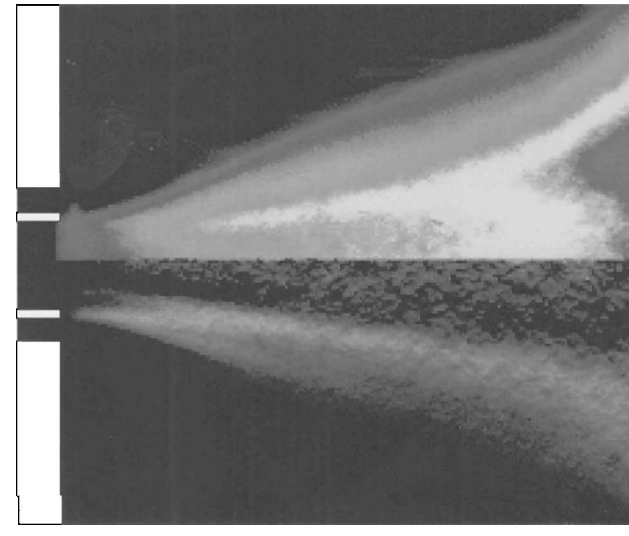

Fig. 11 OH-imaging pictures: line of sight (top) and two-dimensional cross section (bottom); injector near region, image size: 20 × 16 mm.

diameter $d_i = 1.9$ mm, outer diameter $d_a = 2.8$ mm, and a coaxial slit $y = 0.2$ mm (see Fig. 9). The change in the atomization mechanism at reduced surface tension is evident: spray formation at low pressure and dense–light fluid turbulent mixing at a supercritical pressure condition. The critical mixing temperature of the N2/He system is 125.7 K. In the mixing layer between LN2 and He, transcritical zones may exist. The visible surface of the LN2 jet is assumed to be the layer that reached the critical mixing temperature. The effect of surface tension compared to shear forces seems to be negligible. For the experimental setup and more experimental results see Ref. 6.

As shown in experimental studies presented in the next section, the flame surrounds the oxygen jet during injection with a flame temperature of around 3500 K. Additionally, the reaction product H2O will influence the boundary between liquid oxygen and gaseous hydrogen. Computations of the authors of Refs. 10 and 14 indicate that water vapor possibly prevents a phase equilibrium. This point is still not understood to a satisfactory degree, and further research has to be done. The experimental evidence[5] shows that the effect of surface tension compared to shear forces on atomization and mixing under real engine conditions (steady state, high pressure) is negligible.

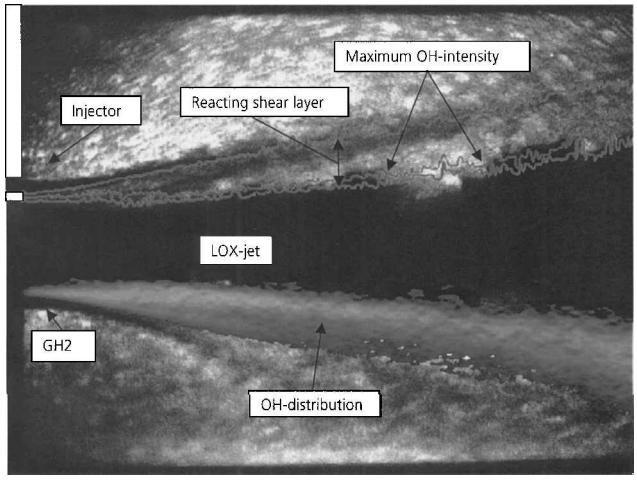

Fig. 12 Shadowgraphy and OH imaging; injector near region, image size: 28 × 21 mm; OH distribution, maximum OH intensity, and reacting shear layer thickness.

Flow and Flame Interaction

The aim of this study is to investigate the flow and flame phenomenology inside the combustion chamber. The experiments were performed with a windowed combustor, as shown in Fig. 10. It consists of an injector head with a single shear coaxial element, a circular combustion chamber, with a length and diameter of 430 mm and 50 mm, respectively, and a variable (exchangeable) nozzle. The combustor is designed for a maximal chamber pressure of 10 MPa and has four windows for optical access. The windows are cooled by a layer of GH2. The cooling flow exits from a coaxial slit parallel to the inner chamber wall. This flow also simulates the kinematic boundary condition of neighboring injector elements that can be found in real rocket engines. The injector baseline dimensions were an outer diameter $d_a = 6.5$ mm and a LOX post inner diameter $d_i = 4$ mm with a LOX post tip wall thickness $y = 0.3$ mm (see Fig. 9).

Shadow photography was used to visualize the oxygen and the hydrogen jet. The strong self-emission of the flame required the use of a special optical setup for shadowgraphy.[5] OH-imaging methods were used to detect the combustion zones.

The window for the optical access has a length of 100 mm and a height of 25 mm. The LOX and GH2 injection temperatures were 127 and 125 K, respectively. The pressure in the combustion chamber was 6.3 MPa. The injection velocities for oxygen and hydrogen were 25 and 301 m/s, respectively. The injector mixture ratio was 5.0 with a hydrogen and oxygen mass flow of 60 and 300 g/s, respectively. The film cooling hydrogen mass flow was 230 g/s and entered the combustor at a velocity of 307 m/s through a 1-mm coaxial slit parallel to the inner chamber wall.

From the flame emission a charge-coupled device (CCD) camera detected the OH-emission wavelength range $\Delta\lambda = 300$–310 nm.

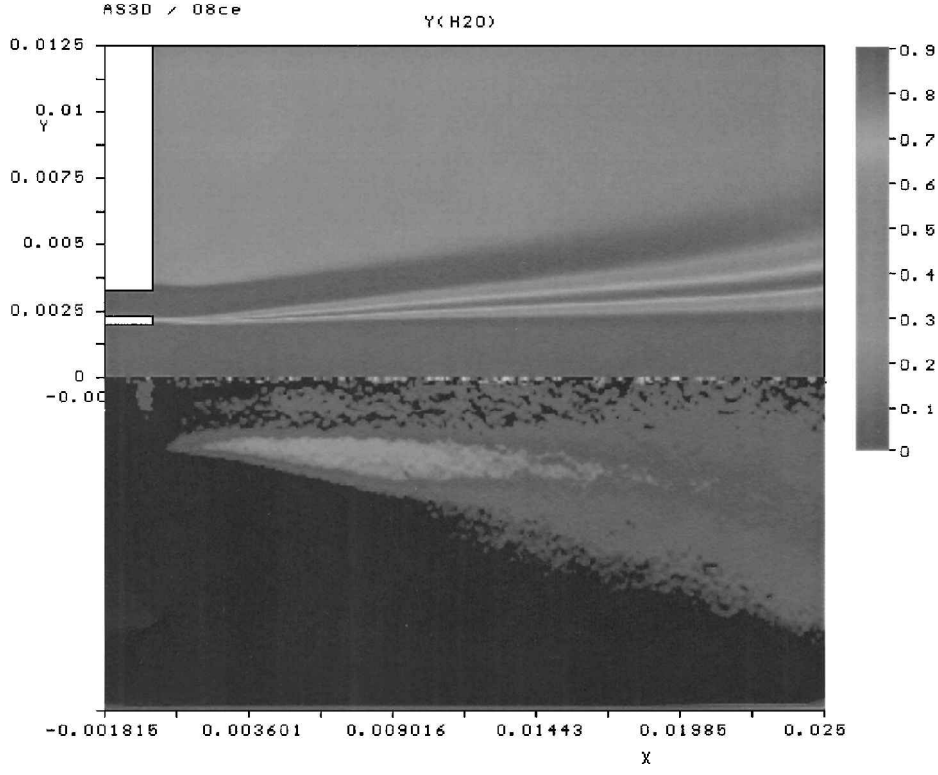

Fig. 13 Comparison between numerical simulation (top) and OH imaging (bottom); injector near region, image size: 20 × 16 mm.

The gate time, that is, the electronic shutter time of the CCD-camera was adjusted to 100 ns, and the frequency of the single shots was 25 Hz. The OH-emission intensity data were transformed using an Abel transformation to produce a two-dimensional cross section through the symmetry line. The Abel transformation assumes cylinder symmetry of the flame. Because the single shots are nonsymmetric due to flow fluctuations, 64 pictures were added to give an average picture. The averaged image is cylinder symmetric, and the Abel transformation can be applied. The upper flow picture of Fig. 11 shows a line-of-sight view and the lower an Abel transformed, two-dimensional, cross section of the near injector region (20 mm length), respectively.

Observed that the flame is attached at the LOX post and that the OH zones are broadening downstream. Figure 12 shows a shadowgraph together with the Abel transformed OH image. It shows that the highest OH intensities are very close to the LOX jet. No ligament or droplet formation can be observed. The heat transfer through the flame to the surface or boundary of the oxygen jet causes a temperature increase to the critical mixing temperature. The surface becomes stringy. The mixing between a dense and a light fluid in a turbulent shear layer takes place.

In addition to the experiments, numerical simulations were done. The principal aim is to validate the assumption that, in rocket combustors, a spray formation does not take place, but rather a dense–light gas mixing conditions exists. The computational fluid dynamics code Aeroshape 3D was utilized, which includes the standard k–e model for turbulence. The combustion is modeled with the assumption of chemical equilibrium using real gas properties for the LOX. Figure 13 shows a comparison between the experimental OH emission and the OH mass fraction of the computation. The calculation was steady and two dimensional.

The numerical mesh has 23,000 cells, and the grid is adaptive to the solution. A calibration of the OH experiment is not possible and so this comparison is qualitative in nature. The legend with the OH mass fractions is only valid for the numerical simulation (top part of Fig. 13). Two major discrepancies are visible. The thickness of the OH zones is not simulated correctly, and the radial distance of the OH zones to the centerline is different between the calculation and experiment. These discrepancies are assumed to be due to the simplified combustion model, although the flame attachment at the LOX post is simulated correctly. The reaction rate is very fast despite the low temperatures of the propellants. Furthermore, the fluid–fluid mixing model seems to give reasonable results without the need for an atomization (spray) model.

Ignition Transients

The aim of this study is to visualize and to analyze the flow and flame transients during engine ignition. Very low hydrogen temperature ignition and combustion instability are of primary concern. Ignition poses many problems to launch vehicles. Late ignition results in hard engine start with high chamber pressure peaks. Total failures of launch missions have been encountered due to ignition problems, for example, ARIANE Flight 18, 1986.[15]

A special experimental setup has been developed to study the processes during ignition in a LOX/GH2 rocket combustor. A windowed combustor with large optical access of 150×30 mm was used. Early tests failed because condensed water vapor contaminated the optical windows in the initial phase, where the window temperature was under the boiling temperature of the combustion product water. Therefore, the model combustor received a window heating device.

The igniter (oxygen–hydrogen pilot burner) was mounted at the center of the chamber 4 cm downstream of the injector plate. The other features of the combustor are shown in Fig. 10. Injector baseline dimensions are a LOX post inner diameter $d_i = 1.2$ mm, outer diameter $d_a = 7$ mm, and a coaxial slit $y = 2.5$ mm (see Fig. 9).

It was very difficult to visualize the ignition process with sufficiently high frequency. At least 10^5 frames/s proved to be necessary. The start of ignition fluctuates (in this study typically ± 10 ms) due to fluctuation of valve opening time (opening time 5 ms) and mixing time. The ignition tests showed that fluctuations in the igniter temperature influenced the onset of ignition considerably. The number of frames of the high-speed camera equipment is limited to around 100. Therefore, the onset of ignition had to be caught exactly, and several tests were necessary to visualize the ignition process.

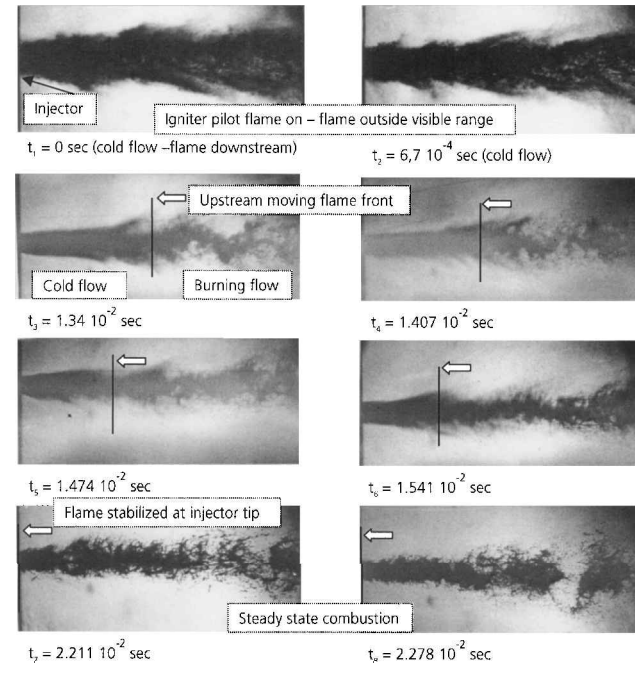

Fig. 14 LOX/GH2 jet: cold-flow (top row), during ignition (two middle rows), and steady-state combustion (bottom row); $p_c = 0.18$ MPa, $u_{LOX} = 14$ m/s, $u_{GH2} = 340$ m/s, $T_{LOX} = 77$ K, and $T_{GH2} = 200$ K.

Figure 14 shows a high-speed sequence of the ignition process. Backlighting illuminated the LOX jet behavior. A short-pulse, high repetition rate flash lamp (High Speed Photo Systeme, Wedel, Germany) illuminated the flowfield with a pulse duration of less than 50 ns.

The top row of Fig. 14 shows the LOX/GH2 injection before ignition. A thick spray of fine LOX droplets is visible with a large divergent spray angle. The two middle rows of Fig. 14 show the upstream movement of the flame indicated through the diminishing of the spray angle and the droplet density. Small droplets cannot be found inside the flame. The observed flame propagation relative to the LOX jet is on the average 0.5–1.0 m/s. Therefore, the absolute propagation velocity is on the order of 10–10^2 m/s. The bottom row of Fig. 14 already shows steady-state combustion conditions. At combustion conditions, the LOX spray consists of a very small amount of ligaments and drops, which rapidly vaporize. The effect of the flame on the LOX jet can be seen in more detail in Fig. 15.

Under cold-flow conditions, very fine liquid oxygen droplets are visible, which are accelerated by aerodynamic forces from the fast flowing hydrogen. After ignition, only large ligaments remain visible. The remarkable smoothness of the LOX jet under combustion conditions is partly due to the rapid vaporization of the oxygen surface waves. It can also be attributed to the density of the hot reaction zone (3500 K) being very low, especially at low chamber pressures. This causes a considerable reduction of aerodynamic interaction between the LOX jet and hydrogen and is indicated by the change of curvature of the jet ligaments at the outer jet surface. In the cold-flow case, the jet surface shows forward swept droplet bursts, whereas under the combustion condition, the oxygen ligaments are bowed backward indicating LOX is faster than the ambient gas. In the latter case, the production of a fine spray is suppressed, and the ligaments are even larger than in the cold-flow case.

The combustion product water may also influence the phase equilibrium, that is, surface tension, and thereby the atomization and mixing process. We can conclude that, with high heating rates, diffusion processes predominate before atomization. This conclusion is only valid for the low-pressure case chosen for this ignition study.

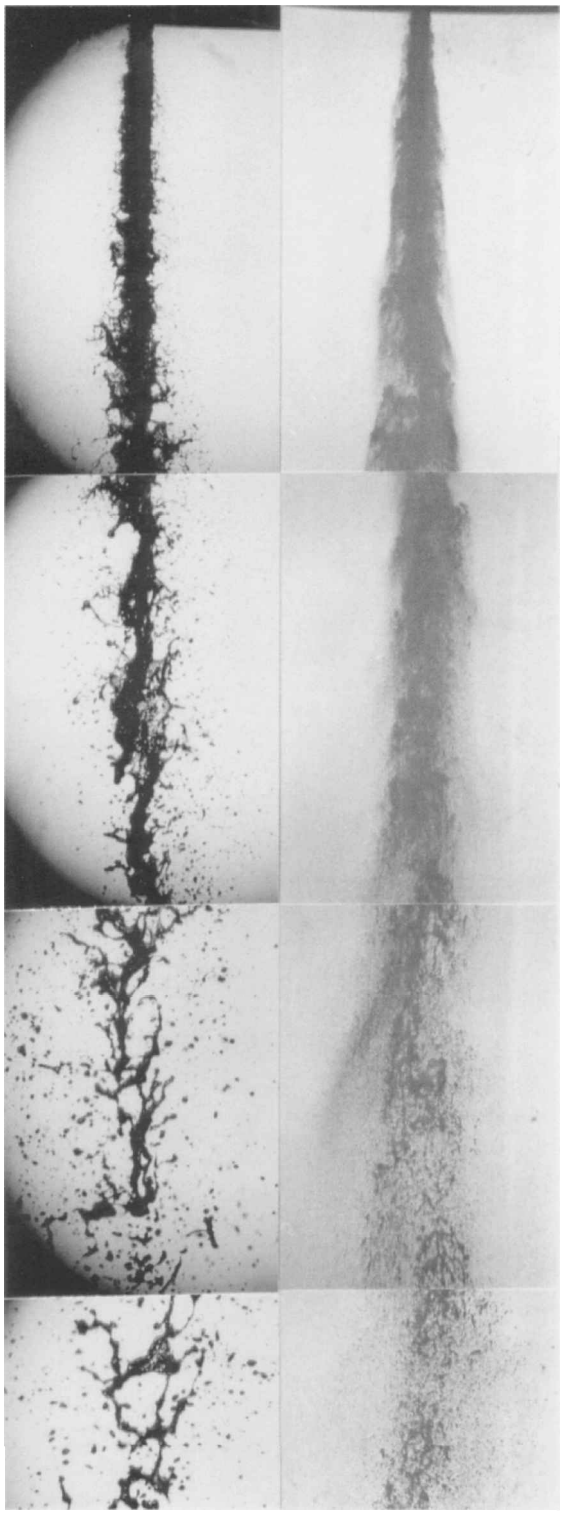

Fig. 15 LOX/GH2 jet: cold-flow (right) and burning (left), p_c = 0.18 MPa, u_{LOX} = 14 m/s, u_{GH2} = 340 m/s, T_{LOX} = 77 K, and T_{GH2} = 200 K.

Summary and Conclusions

The experimental and theoretical studies show that heat flux and temperature dominantly affect the mixing behavior near and above the critical pressure. The strong difference between atomization with and in absence of surface tension has been pointed out. It seems that the effect of capillary forces on atomization and mixing under real engine conditions (steady state, high pressure) is negligible. This is in agreement with the experimental observations, where droplet formation was not observed in this rocket engine at pressures near or above the supercritical pressure. The hot-fire tests revealed that the reacting shear layer between the propellants strongly affects the mixing process. Because of the low density of the flame gases, the aerodynamic effect on atomization is diminished compared to the cold-flow case. The ignition tests demonstrated the change of the mixing mechanisms before and after ignition. In the hot-fire case, the production of a fine spray is suppressed; the ligaments are larger than in the cold-flow case. The absolute flame propagation speed is on the order of $10–10^2$ m/s.

Acknowledgments

This work is supported within the framework of the German National Technology Programme Cryogenic Rocket Engines, by the German Ministry of Education and Research (BMBF) under Contract 50TT9628. We thank the M3 and P8 test bench teams for realization of the hot-fire test. Technical support of G. Schneider is highly appreciated.

References

[1]Immich, H., and Mayer, W., "Cryogenic Liquid Rocket Engine Technology Developments Within the German National Technology Programme," AIAA Paper 97-2822, July 1997.

[2]Mayer, W., "TEKAN—Research on Cryogenic Rocket Engines at DLR Lampoldshausen," AIAA Paper 2000-3219, July 2000.

[3]Mayer, W., Schik, A., Vieille, B., Chaveau, C., Goekalp, I., Talley, D., and Woodward, R., "Atomization and Breakup of Cryogenic Propellants under High-Pressure Subcritical and Supercritical Conditions," *Journal of Propulsion and Power*, Vol. 14, No. 5, 1998, pp. 835–842.

[4]Mayer, W., "Coaxial Atomization of a Round Liquid Jet in a High Speed Gas Stream: A Phenomenological Study," *Experiments in Fluids*, Vol. 16, No. 6, 1994, pp. 401–410.

[5]Mayer, W., and Tamura, H., "Propellant Injection in a Liquid Oxygen/Gaseous Hydrogen Rocket Engine," *Journal of Propulsion and Power*, Vol. 12, No. 6, 1996, pp. 1137–1147.

[6]Mayer, W., Schik, A., Schaeffler, M., and Tamura, H., "Injection and Mixing Processes in High Pressure Liquid Oxygen/Gaseous Hydrogen Rocket Combustors," *Journal of Propulsion and Power*, Vol. 15, No. 5, 2000, pp. 823–828.

[7]Woodward, R. D., and Talley, D. G., "Raman Imaging of Transcritical Cryogenic Propellants," AIAA Paper 96-0468, Jan. 1996.

[8]Lefebvre, A., *Atomization and Sprays*, Hemisphere, New York, 1989, pp. 37–58.

[9]Delplanque, J.-P., and Sirignano, W. A., "Numerical Study of the Transient Vaporization of an Oxygen Droplet at Sub- and Supercritical Conditions," *International Journal of Heat and Mass Transfer*, Vol. 36, 1993, pp. 303–314.

[10]Litchford, R. J., and Jeng, S.-M., "LOX Vaporization in High-Pressure, Hydrogen-Rich Gas," AIAA Paper 90-2191, 1990.

[11]Macleod, D. B., *Transactions of the Faraday Society*, Vol. 19, 1923, p. 38.

[12]Sudgen, S., "The Variation of Surface Tension with Temperature," *J. Chem. Soc.*, 1924, pp. 32–41.

[13]Sudgen, S., "A Relation Between Surface Tension, Density and Chemical Composition," *J. Chem. Soc.*, 1924, pp. 1177–1183.

[14]Daou, J., Haldenwang, P., and Nicoli, C., "Supercritical Burning of Liquid Oxygen (LOX) Droplet with Detailed Chemistry," *Combustion and Flame*, Vol. 101, 1995, pp. 153–169.

[15]Gastal, J., "ARIANE Third Stage Ignition Improvement," AIAA Paper 88-2932, July 1988.